

A New Class of Atomically Precise, Hydride-Rich Silver Nanoclusters Co-Protected by Phosphines

Megalamane S. Bootharaju,^{†,‡} Raju Dey,[‡] Lieven E. Gevers,[‡] Mohamed N. Hedhili,[§] Jean-Marie Basset,[‡] and Osman M. Bakr^{*,†}

[†]Division of Physical Sciences and Engineering, KAUST Solar Center, [‡]KAUST Catalysis Center (KCC), and [§]Imaging and Characterization Laboratory, King Abdullah University of Science and Technology (KAUST), Thuwal 23955-6900, Saudi Arabia

S Supporting Information

ABSTRACT: Thiols and phosphines are the most widely used organic ligands to attain atomically precise metal nanoclusters (NCs). Here, we used simple hydrides (e.g., H⁻) as ligands along with phosphines, such as triphenylphosphine (TPP), 1,2-bis(diphenylphosphino)ethane [DPPE], and tris(4-fluorophenyl)phosphine [TFPP] to design and synthesize a new class of hydride-rich silver NCs. This class includes [Ag₁₈H₁₆(TPP)₁₀]²⁺, [Ag₂₅H₂₂(DPPE)₈]³⁺, and [Ag₂₆H₂₂(TFPP)₁₃]²⁺. Our work reveals a new family of atomically precise NCs protected by H⁻ ligands and labile phosphines, with potentially more accessible active metal sites for functionalization and provides a new set of stable NC sizes with simpler ligand–metal bonding for researchers to explore both experimentally and computationally.

It is now possible to manipulate a material's properties through atom-by-atom arrangement.^{1–5} The organization of as few as 10, and up to a several hundred, metal atoms into unique structures that are protected by a definite number of ligands has enabled the development of a new class of functional materials called atomically precise nanoparticles (NPs), or nanoclusters (NCs).^{6–10} These compositionally precise materials are also known as molecular NPs as a result of their molecule-like optical,^{11,12} photophysical,^{13,14} chemical,^{15–17} and electronic properties.^{18,19} These properties have given rise to promising applications in catalysis,²⁰ energy conversion,⁶ and environmental remediation.⁶

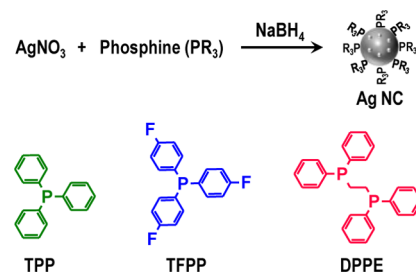
Among all NCs, the ligand-protected ones of noble metals, particularly Au^{1,8} and Ag,^{2,7} have been widely investigated. The classic ligands used for the synthesis of these NCs are organic, including thiols,^{1,21} phosphines,²² and/or their combination.²³ The structures of those ligands have been developed to stabilize a large number of NCs, including Au₁₈,²⁴ Au₂₅,²⁵ and Au₁₀₂²⁶ in gold; Ag₁₄,²⁷ Ag₁₆,²⁸ Ag₂₁,²⁹ Ag₂₅,³⁰ Ag₂₉,³ Ag₃₂,²⁸ and Ag₄₄^{31,32} in silver; and MAg₂₄ (M = Au, Pd or Pt),^{18,19} and Ag₃₂Au₁₂³² in alloys. In contrast, other types of ligands, e.g., inorganic ones that include simple ions (e.g., H⁻, HS⁻, and OH⁻) have rarely been used in the synthesis of Au³³ and Ag³⁴ NCs and are a minor fraction of the ligand-shell in those rare cases. Remarkably, these simple and short ionic ligands were found to be important on the surfaces of quantum dots by increasing the charge transport that facilitates device performance.³⁵ Use of such atomic ligands for Au and Ag would offer opportunities

to explore the development of new sizes of NCs with innovative and enhanced properties for optoelectronic and catalytic applications.

The dearth of reports on using inorganic short ligands in forming NCs reflects difficulties in the overall synthesis. The stabilization of NCs provided by short ligands seems to be inadequate, and extra protection through coligands such as phosphines or thiols is likely necessary. Among several short ligands, the hydride (H⁻), a spherical closed-shell anion,³⁶ was used along with phosphine coligands in the synthesis of a few Cu^{37,38} and Ag^{34,39} NCs, where these low-nuclearity Ag NCs contain only a few hydrides. These do not fully afford the NCs with the potential advantages of the H⁻ ligand and cannot serve as practical containers for hydrogen^{34,36} or model systems for Ag-hydrides that are found to be key intermediates in organic reactions.⁴⁰

Given the advantages of using hydrides as ligands, we designed a reaction (Scheme 1) to synthesize a new class of Ag

Scheme 1. Synthesis of Ag NCs (top) Using Phosphine Ligands (bottom) of Different Molecular Structures



NCs with hydrides as the majority ligand. In our reaction, NaBH₄ plays a dual role as both a reducing agent and a source of H⁻. Along with H⁻, we used labile phosphines (which are more weakly bound to clusters than thiols) both to stabilize the NCs and as a lever to tune their sizes. We find that under the same experimental conditions, a new set of H⁻-rich Ag NCs could be synthesized, namely Ag₁₈, Ag₂₅ and Ag₂₆, by using different phosphine structures with single or multiple binding sites, such as triphenylphosphine (TPP), 1,2-bis(diphenylphosphino)ethane [DPPE], and tris(4-fluorophenyl)phosphine [TFPP], respectively (Scheme 1).

Received: May 27, 2016

Published: October 10, 2016

Typical synthesis of Ag NCs involves the addition of a Ag precursor in methanol (MeOH) to a phosphine in dichloromethane (DCM). After that, aqueous sodium borohydride (NaBH_4) was added to produce Ag NCs protected by hydrides and phosphines together (see the Supporting Information (SI) for details).

The NCs formed with TPP appeared dark green in MeOH (inset of Figure 1A). Its UV-vis spectrum (Figure 1A) shows a

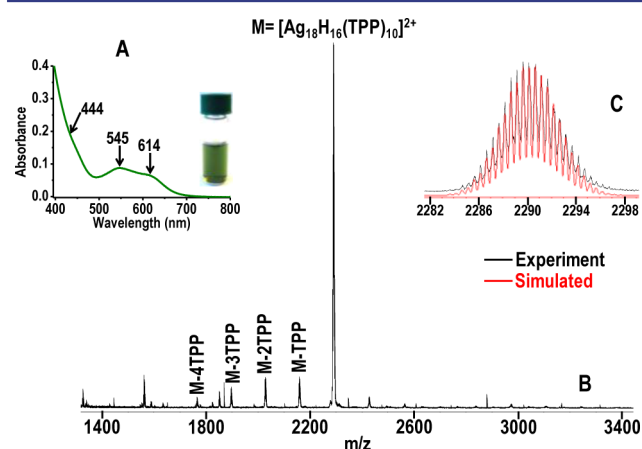


Figure 1. (A) UV-vis absorption and (B) positive-mode ESI MS of $[\text{Ag}_{18}\text{H}_{16}(\text{TPP})_{10}]^{2+}$ NCs. Inset of A: a photograph of the cluster in MeOH. (C) Comparison of experimental and simulated mass spectra of $[\text{Ag}_{18}\text{H}_{16}(\text{TPP})_{10}]^{2+}$.

continuous broad absorption in the 500–650 nm region with two distinct features at 545 and 614 nm with a shoulder peak at 444 nm. This spectrum is contrast to the absorption spectrum of TPP-stabilized plasmonic Ag NPs (AgTPP NPs), which has a sharp peak at 408 nm (Figure S1). Moreover, AgTPP NP solution is light yellow. The absence of a plasmonic absorption feature, the green appearance, and the molecular optical signatures together suggest that our synthesized product has a molecule-like character.

To identify the molecular formula and the nature of the charge-state of the NCs, we used electrospray ionization mass spectrometry (ESI MS), a mass analysis tool with soft ionization. The ESI MS of the cluster, in positive ion mode, shows two intense peaks of $[\text{Ag}(\text{TPP})_2]^+$ and $[\text{Ag}(\text{TPP})_3]^+$ (Figure S2) along with a peak at $m/z \sim 2290$ (Figure 1B). A close inspection of the latter peak reveals a characteristic Ag isotopic pattern, where peaks are separated by m/z 0.5 (Figure 1C), indicating a cluster charge of +2. By considering all possibilities, we identified the composition of $m/z \sim 2290$ peak as $[\text{Ag}_{18}\text{H}_{16}(\text{TPP})_{10}]^{2+}$. An exact match of isotopic pattern of this peak with a simulated mass spectrum of $[\text{Ag}_{18}\text{H}_{16}(\text{TPP})_{10}]^{2+}$ unambiguously confirmed (Figure 1C) that the cluster is $[\text{Ag}_{18}\text{H}_{16}(\text{TPP})_{10}]^{2+}$. Besides the $m/z \sim 2290$ peak, other peaks separated by m/z 131 (i.e., 262/2) are also apparent due to sequential loss of TPP (Figure 1B), which is common in Ag-phosphine NCs due to their weak bonding to the cluster.³

Although we were able to reliably assign the cluster's formula, we also sought to verify the presence and the number of hydrides. For this purpose, we synthesized the cluster with NaBD_4 (see SI) to observe NCs without hydrides. The color and the UV-vis spectrum of the NCs (Figure S3) were very similar to $[\text{Ag}_{18}\text{H}_{16}(\text{TPP})_{10}]^{2+}$. The ESI MS shows a peak at $m/z \sim 2298$ (Figure S4), which is shifted by $m/z \sim 8$ toward higher mass from $[\text{Ag}_{18}\text{H}_{16}(\text{TPP})_{10}]^{2+}$, confirming the presence of hydrides in the original cluster. The experimental mass spectrum was found to match with a simulated spectrum of $[\text{Ag}_{18}\text{D}_{16}(\text{TPP})_{10}]^{2+}$ (Figure S4). ^1H , ^2H , and ^{31}P nuclear magnetic resonance (NMR) analysis of $[\text{Ag}_{18}\text{H}_{16}(\text{TPP})_{10}]^{2+}$ and its deuterated analogue further substantiates the presence of hydrides and deuterides, respectively (Figures S5,6). Variable-temperature (VT) NMR of $[\text{Ag}_{18}\text{H}_{16}(\text{TPP})_{10}]^{2+}$ indicates different orientations of TPP at low temperatures (Figure S7). Upon heating the $[\text{Ag}_{18}\text{H}_{16}(\text{TPP})_{10}]^{2+}$, H_2 gas was found to be released (Figure S8), a typical character of metal hydrides.⁴¹ Note that TPP+ NaBH_4 control and AgTPP complex (Figures S9,10) did not produce H_2 . These experiments strongly indicate the presence of hydrides in $[\text{Ag}_{18}\text{H}_{16}(\text{TPP})_{10}]^{2+}$ cluster. Scanning electron microscopy energy-dispersive X-ray spectroscopy and X-ray fluorescence analysis of $[\text{Ag}_{18}\text{H}_{16}(\text{TPP})_{10}]^{2+}$ confirmed the presence of elements Ag and P with Ag:P atomic ratios that are close to the Ag:P atomic ratio in the cluster (Figure S11).

It is worth noting that the ESI MS peak at $m/z \sim 2290$ is close to another composition of $[\text{Ag}_{17}(\text{NO}_3)_2(\text{TPP})_{10}]^{2+}$ in addition to $[\text{Ag}_{18}\text{H}_{16}(\text{TPP})_{10}]^{2+}$. The NO_3^- , from AgNO_3 during synthesis, can act as a ligand for the cluster similar to some Au NCs.⁴² To resolve this compositional ambiguity, we prepared a NC by replacing the Ag precursor AgNO_3 with CF_3COOAg . Both the ESI MS and UV-vis (Figure S12) of this cluster were identical to those NCs obtained from AgNO_3 (Figure 1), clearly revealing the absence of an anion effect on the composition of the cluster and, importantly, the absence of CF_3COO^- or NO_3^- in the cluster.

To explore the effect of the phosphine's structure on the NC's size, we used another phosphine, TFPP, where three para H atoms of TPP were replaced by three F atoms (Scheme 1). The synthesis of the NCs is similar to Ag_{18} except for the replacement of TPP with TFPP (see SI). Remarkably, like Ag_{18} , the AgTFPP cluster solution was also green (inset of Figure 2A). The optical spectrum was similar to that of Ag_{18} in 500–700 nm range (Figure 2A). However, we noted a distinct change in the 350–480 nm region, in which two well-defined peaks are apparent at 394 and 438 nm, suggesting the formation of another size Ag NC.

Figure 2. (A) UV-vis absorption spectrum of $[\text{Ag}_{26}\text{H}_{22}(\text{TFPP})_{13}]^{2+}$ NCs showing peaks at 394, 438, 540, and 620 nm. Inset shows a photograph of the green cluster in MeOH. (B) Positive-mode ESI MS spectrum showing peaks for M-4TFPP, M-3TFPP, M-2TFPP, and M-TFPP, with a major peak at $m/z \sim 3470$. (C) Comparison of experimental (black line) and simulated (red line) mass spectra of $[\text{Ag}_{26}\text{H}_{22}(\text{TFPP})_{13}]^{2+}$.

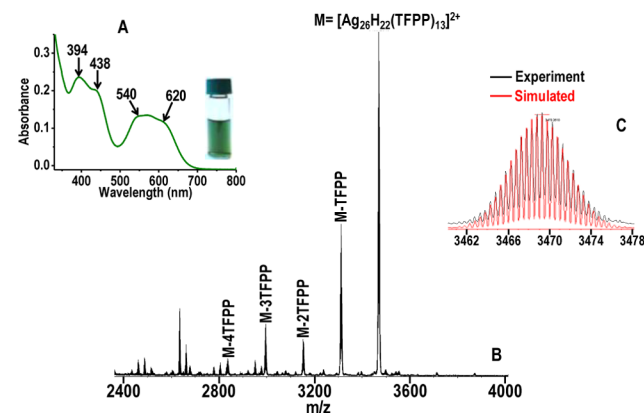


Figure 2. (A) UV-vis absorption and (B) positive-mode ESI MS of $[\text{Ag}_{26}\text{H}_{22}(\text{TFPP})_{13}]^{2+}$ NCs. Inset of A: a photograph of the cluster in MeOH. (C) Comparison of experimental and simulated spectra of $[\text{Ag}_{26}\text{H}_{22}(\text{TFPP})_{13}]^{2+}$.

The ESI MS of the AgTFPP NCs shows peaks of $[\text{Ag}(\text{TFPP})_2]^+$ and $[\text{Ag}(\text{TFPP})_3]^+$ in the low-mass region (Figure S13). An intense peak at $m/z \sim 3469$ was observed in the high-mass region with a peak separation of m/z 0.5, indicating a charge state of +2. The total mass of 6938 (i.e., 3469×2) matches the composition of the $[\text{Ag}_{26}\text{H}_{22}(\text{TFPP})_{13}]^{2+}$ NC (Figure 2B). Furthermore, the experimental data perfectly match with the simulated spectrum of the $[\text{Ag}_{26}\text{H}_{22}(\text{TFPP})_{13}]^{2+}$ formula (Figure 2C). Similar to TPP, other peaks corresponding to the sequential loss of TFPP were also observed, consistent with the proposed composition assignment. The number of hydrides was confirmed by synthesizing NCs by using NaBD₄. The ESI MS reveals the presence of 22D in the Ag₂₆ cluster (Figure S14), indicating that the total number of hydrides in the original cluster is 22. The presence of hydrides in these clusters was further supported by combined ¹H, ²H, ³¹P NMR and H₂-evolution experiments (Figures S15–19), while VT NMR spectra show the re-orientation of TFPP on $[\text{Ag}_{26}\text{H}_{22}(\text{TFPP})_{13}]^{2+}$ surface at low temperatures (Figure S20). The Ag:P atomic ratio of $[\text{Ag}_{26}\text{H}_{22}(\text{TFPP})_{13}]^{2+}$ was in good agreement with the Ag:P atomic ratios obtained from elemental analysis of this cluster (Figure S21).

These experimental findings show that a slight variation in the phosphine's structure can result in a dramatic difference in the NC's size. To substantiate this hypothesis further, we chose another category of phosphines with two binding sites (e.g., DPPE, Scheme 1), unlike TPP and TFPP with single binding site. The synthesis of NCs was similar to those of Ag₁₈ and Ag₂₆ but in the presence of DPPE (see SI). While the Ag₁₈ and Ag₂₆ appeared green, AgDPPE cluster was orange (inset of Figure 3A). The optical spectrum (Figure 3A) shows two peaks at 545 and 460 nm, suggesting the formation of a new Ag NC with DPPE.

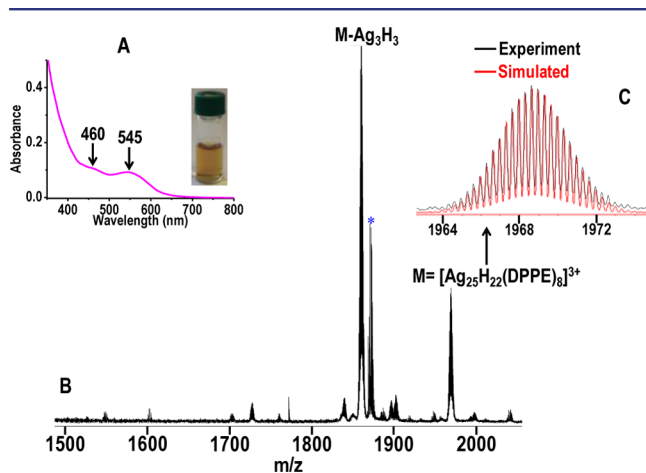


Figure 3. (A) UV-vis absorption and (B) positive-mode ESI MS of $[\text{Ag}_{25}\text{H}_{22}(\text{DPPE})_8]^{3+}$ NCs. Inset of A: a photograph of the cluster in MeOH. (C) Comparison of experimental and simulated spectra of $[\text{Ag}_{25}\text{H}_{22}(\text{DPPE})_8]^{3+}$. The * peak corresponds to a byproduct, $[\text{Ag}_2\text{B}(\text{OH})_3(\text{DPPE})_4]^+$ (Figure S33).

The ESI MS of the AgDPPE NC (Figure 3B) shows a peak at $m/z \sim 1969$. Expansion of this peak reveals a peak separation of m/z 0.33 (Figure 3C), indicating a charge of the species to be +3. The total mass of 5907 corresponds to a molecular mass of the $[\text{Ag}_{25}\text{H}_{22}(\text{DPPE})_8]^{3+}$ NC. Overlap of experimental data with a simulated mass spectrum for $[\text{Ag}_{25}\text{H}_{22}(\text{DPPE})_8]^{3+}$

validated this formula (Figure 3C). Unlike in Ag₁₈ and Ag₂₆, no sequential loss of DPPE was observed in Ag₂₅. However, an intense peak of $[\text{Ag}_{22}\text{H}_{19}(\text{DPPE})_8]^{3+}$ was noticed (Figure S22), likely due to the fragmentation of the parent $[\text{Ag}_{25}\text{H}_{22}(\text{DPPE})_8]^{3+}$ by a loss of Ag₃H₃. The number of hydrides in $[\text{Ag}_{25}\text{H}_{22}(\text{DPPE})_8]^{3+}$ and in its fragment $[\text{Ag}_{22}\text{H}_{19}(\text{DPPE})_8]^{3+}$ was verified by preparing the NCs using NaBD₄. ESI MS revealed a mass shift by $m/z \sim 7.33$ and ~ 6.33 , respectively, for $[\text{Ag}_{25}\text{H}_{22}(\text{DPPE})_8]^{3+}$ and $[\text{Ag}_{22}\text{H}_{19}(\text{DPPE})_8]^{3+}$, confirming the presence of 22 and 19D to account for the $[\text{Ag}_{25}\text{D}_{22}(\text{DPPE})_8]^{3+}$ and $[\text{Ag}_{22}\text{D}_{19}(\text{DPPE})_8]^{3+}$ compositions, respectively (Figures S23,24). In addition, ¹H and ²H NMR and H₂-liberation (Figures S25–29) all confirm the actual presence of hydrides in the $[\text{Ag}_{25}\text{H}_{22}(\text{DPPE})_8]^{3+}$ NCs. In contrast to Ag₁₈ and Ag₂₆, VT NMR data of $[\text{Ag}_{25}\text{H}_{22}(\text{DPPE})_8]^{3+}$ (Figure S30) show the unsplit ³¹P NMR signals, suggesting DPPE's rigidity, which restricts its re-orientation on the NC surface at low temperatures. Furthermore, the Ag:P atomic ratio of $[\text{Ag}_{25}\text{H}_{22}(\text{DPPE})_8]^{3+}$ was consistent with the elemental analysis (Figure S31). X-ray photoelectron spectroscopy (XPS) (Figure S32) of all NCs reveals the oxidation state of Ag close to Ag(0).⁴³

The $[\text{Ag}_{18}\text{H}_{16}(\text{TPP})_{10}]^{2+}$ formula is close to a Cu NC³⁷ of $[\text{Cu}_{18}\text{H}_{17}(\text{TPP})_{10}]^+$ with only a difference in the charge and the number of hydrides. The electron count rule² suggests that $[\text{Ag}_{18}\text{H}_{16}(\text{TPP})_{10}]^{2+}$ and $[\text{Ag}_{25}\text{H}_{22}(\text{DPPE})_8]^{3+}$ possess zero free valence electrons, while $[\text{Ag}_{26}\text{H}_{22}(\text{TFPP})_{13}]^{2+}$ has two electrons. The Ag₂₆ is believed to exhibit stability by following an electronic close-shell rule,^{2,44,45} while the stabilities of Ag₁₈ and Ag₂₅ could be attributed to inherent geometric factors. Based on the fact of direct bonding of phosphines to Ag or Au atoms of NCs, the metal cores (with hydrides) of Ag₁₈, Ag₂₆, and Ag₂₅ are predicted to be Ag₈, Ag₁₃, and Ag₉, respectively. The recently reported $[\text{Cu}_{25}\text{H}_{22}(\text{TPP})_{12}]^+$ has 12-monodentate TPP ligands,³⁷ while our Ag₂₅ possesses eight bidentate DPPE ligands with 16 binding sites, inferring that their crystal structures are different. It will be essential to determine crystal structures of our NCs in the near future to reveal the arrangement of Ag atoms and ligands and fully elucidate the origins of their stability.

In summary, we reported the synthesis and identification of a new class of hydride-rich, atomically precise Ag NCs. This class includes Ag₁₈, Ag₂₅, and Ag₂₆, which have phosphines as coprotectors. The NCs exhibit molecule-like optical features, and their compositions were determined through high-resolution ESI MS, elemental analysis, NMR, XPS, and several control experiments. The small size of the hydrides combined with the labile nature of phosphines on the NCs may provide active sites that are promising for catalytic application. Our successful demonstration of tuning the NC size, optical properties, and electronic charge pave the way for the use of smaller ionic ligands to further explore the distinct and unique sizes of various metal NCs.

■ ASSOCIATED CONTENT

Supporting Information

The Supporting Information is available free of charge on the ACS Publications website at DOI: 10.1021/jacs.6b05482.

Details of synthesis and characterization of NCs (PDF)

■ AUTHOR INFORMATION

Corresponding Author

*osman.bakr@kaust.edu.sa

Notes

The authors declare no competing financial interest.

■ ACKNOWLEDGMENTS

Funding for this work was provided by KAUST.

■ REFERENCES

- (1) Jin, R. *Nanoscale* **2015**, *7*, 1549.
- (2) Joshi, C. P.; Bootharaju, M. S.; Bakr, O. M. *J. Phys. Chem. Lett.* **2015**, *6*, 3023.
- (3) AbdulHalim, L. G.; Bootharaju, M. S.; Tang, Q.; Del Gobbo, S.; AbdulHalim, R. G.; Eddaoudi, M.; Jiang, D.-e.; Bakr, O. M. *J. Am. Chem. Soc.* **2015**, *137*, 11970.
- (4) Salorinne, K.; Malola, S.; Wong, O. A.; Rithner, C. D.; Chen, X.; Ackerson, C. J.; Häkkinen, H. *Nat. Commun.* **2016**, *7*, 10401.
- (5) Tofanelli, M. A.; Ni, T. W.; Phillips, B. D.; Ackerson, C. J. *Inorg. Chem.* **2016**, *55*, 999.
- (6) Mathew, A.; Pradeep, T. *Part. Part. Syst. Charact.* **2014**, *31*, 1017.
- (7) Zheng, K.; Yuan, X.; Goswami, N.; Zhang, Q.; Xie, J. *RSC Adv.* **2014**, *4*, 60581.
- (8) Kurashige, W.; Niihori, Y.; Sharma, S.; Negishi, Y. *J. Phys. Chem. Lett.* **2014**, *5*, 4134.
- (9) Petty, J. T.; Sergev, O. O.; Ganguly, M.; Rankine, I. J.; Chevrier, D. M.; Zhang, P. *J. Am. Chem. Soc.* **2016**, *138*, 3469.
- (10) Ruiz Aranzaes, J.; Belin, C.; Astruc, D. *Chem. Commun.* **2007**, 3456.
- (11) Negishi, Y.; Nakazaki, T.; Malola, S.; Takano, S.; Niihori, Y.; Kurashige, W.; Yamazoe, S.; Tsukuda, T.; Häkkinen, H. *J. Am. Chem. Soc.* **2015**, *137*, 1206.
- (12) Goswami, N.; Yao, Q.; Luo, Z.; Li, J.; Chen, T.; Xie, J. *J. Phys. Chem. Lett.* **2016**, *7*, 962.
- (13) Aly, S. M.; AbdulHalim, L. G.; Besong, T. M. D.; Soldan, G.; Bakr, O. M.; Mohammed, O. F. *Nanoscale* **2016**, *8*, 5412.
- (14) Petty, J. T.; Sergev, O. O.; Kantor, A. G.; Rankine, I. J.; Ganguly, M.; David, F. D.; Wheeler, S. K.; Wheeler, J. F. *Anal. Chem.* **2015**, *87*, 5302.
- (15) Krishnadas, K. R.; Ghosh, A.; Baksi, A.; Chakraborty, I.; Natarajan, G.; Pradeep, T. *J. Am. Chem. Soc.* **2016**, *138*, 140.
- (16) Yao, C.; Chen, J.; Li, M.-B.; Liu, L.; Yang, J.; Wu, Z. *Nano Lett.* **2015**, *15*, 1281.
- (17) Bootharaju, M. S.; Joshi, C. P.; Alhilaly, M. J.; Bakr, O. M. *Chem. Mater.* **2016**, *28*, 3292.
- (18) Bootharaju, M. S.; Joshi, C. P.; Parida, M. R.; Mohammed, O. F.; Bakr, O. M. *Angew. Chem.* **2016**, *128*, 934.
- (19) Yan, J.; Su, H.; Yang, H.; Malola, S.; Lin, S.; Häkkinen, H.; Zheng, N. *J. Am. Chem. Soc.* **2015**, *137*, 11880.
- (20) Urushizaki, M.; Kitazawa, H.; Takano, S.; Takahata, R.; Yamazoe, S.; Tsukuda, T. *J. Phys. Chem. C* **2015**, *119*, 27483.
- (21) Negishi, Y.; Arai, R.; Niihori, Y.; Tsukuda, T. *Chem. Commun.* **2011**, *47*, 5693.
- (22) McKenzie, L. C.; Zaikova, T. O.; Hutchison, J. E. *J. Am. Chem. Soc.* **2014**, *136*, 13426.
- (23) Soldan, G.; Aljuhani, M. A.; Bootharaju, M. S.; AbdulHalim, L. G.; Parida, M. R.; Emwas, A.-H.; Mohammed, O. F.; Bakr, O. M. *Angew. Chem., Int. Ed.* **2016**, *55*, 5749.
- (24) Chen, S.; Wang, S.; Zhong, J.; Song, Y.; Zhang, J.; Sheng, H.; Pei, Y.; Zhu, M. *Angew. Chem., Int. Ed.* **2015**, *54*, 3145.
- (25) Zhu, M.; Aikens, C. M.; Hollander, F. J.; Schatz, G. C.; Jin, R. *J. Am. Chem. Soc.* **2008**, *130*, 5883.
- (26) Jadzinsky, P. D.; Calero, G.; Ackerson, C. J.; Bushnell, D. A.; Kornberg, R. D. *Science* **2007**, *318*, 430.
- (27) Yang, H.; Lei, J.; Wu, B.; Wang, Y.; Zhou, M.; Xia, A.; Zheng, L.; Zheng, N. *Chem. Commun.* **2013**, *49*, 300.
- (28) Yang, H.; Wang, Y.; Zheng, N. *Nanoscale* **2013**, *5*, 2674.
- (29) Dhayal, R. S.; Liao, J.-H.; Liu, Y.-C.; Chiang, M.-H.; Kahlal, S.; Saillard, J.-Y.; Liu, C. W. *Angew. Chem., Int. Ed.* **2015**, *54*, 3702.
- (30) Joshi, C. P.; Bootharaju, M. S.; Alhilaly, M. J.; Bakr, O. M. *J. Am. Chem. Soc.* **2015**, *137*, 11578.
- (31) Desireddy, A.; Conn, B. E.; Guo, J.; Yoon, B.; Barnett, R. N.; Monahan, B. M.; Kirschbaum, K.; Griffith, W. P.; Whetten, R. L.; Landman, U.; Bigioni, T. P. *Nature* **2013**, *501*, 399.
- (32) Yang, H.; Wang, Y.; Huang, H.; Gell, L.; Lehtovaara, L.; Malola, S.; Häkkinen, H.; Zheng, N. *Nat. Commun.* **2013**, *4*, 2422.
- (33) Escalle, A.; Mora, G.; Gagosz, F.; Mézailles, N.; Le Goff, X. F.; Jean, Y.; Le Floch, P. *Inorg. Chem.* **2009**, *48*, 8415.
- (34) Zavras, A.; Khairallah, G. N.; Connell, T. U.; White, J. M.; Edwards, A. J.; Donnelly, P. S.; O'Hair, R. A. J. *Angew. Chem., Int. Ed.* **2013**, *52*, 8391.
- (35) Nag, A.; Kovalenko, M. V.; Lee, J.-S.; Liu, W.; Spokoyny, B.; Talapin, D. V. *J. Am. Chem. Soc.* **2011**, *133*, 10612.
- (36) Dhayal, R. S.; van Zyl, W. E.; Liu, C. W. *Acc. Chem. Res.* **2016**, *49*, 86.
- (37) Nguyen, T.-A. D.; Jones, Z. R.; Goldsmith, B. R.; Buratto, W. R.; Wu, G.; Scott, S. L.; Hayton, T. W. *J. Am. Chem. Soc.* **2015**, *137*, 13319.
- (38) Nguyen, T.-A. D.; Goldsmith, B. R.; Zaman, H. T.; Wu, G.; Peters, B.; Hayton, T. W. *Chem. - Eur. J.* **2015**, *21*, 5341.
- (39) Daly, S.; Krstic, M.; Giuliani, A.; Antoine, R.; Nahon, L.; Zavras, A.; Khairallah, G. N.; Bonacic-Koutecky, V.; Dugourd, P.; O'Hair, R. A. *Phys. Chem. Chem. Phys.* **2015**, *17*, 25772.
- (40) Shimizu, K.-i.; Sato, R.; Satsuma, A. *Angew. Chem., Int. Ed.* **2009**, *48*, 3982.
- (41) Dhayal, R. S.; Liao, J.-H.; Lin, Y.-R.; Liao, P.-K.; Kahlal, S.; Saillard, J.-Y.; Liu, C. W. *J. Am. Chem. Soc.* **2013**, *135*, 4704.
- (42) Gutrath, B. S.; Opper, I. M.; Presly, O.; Beljakov, I.; Meded, V.; Wenzel, W.; Simon, U. *Angew. Chem., Int. Ed.* **2013**, *52*, 3529.
- (43) Rao, T. U. B.; Nataraju, B.; Pradeep, T. *J. Am. Chem. Soc.* **2010**, *132*, 16304.
- (44) Walter, M.; Akola, J.; Lopez-Acevedo, O.; Jadzinsky, P. D.; Calero, G.; Ackerson, C. J.; Whetten, R. L.; Grönbeck, H.; Häkkinen, H. *Proc. Natl. Acad. Sci. U. S. A.* **2008**, *105*, 9157.
- (45) Gell, L.; Lehtovaara, L.; Häkkinen, H. *J. Phys. Chem. A* **2014**, *118*, 8351.